Aust. J. Phys., 1977, **30**, 287–301

The Optical Model and Proton Elastic Scattering from ^{14}N and ^{16}O

A. Gabric and K. Amos

School of Physics, University of Melbourne, Parkville, Vic. 3052.

Abstract

Allowing for important doorway state effects in analyses of proton elastic scattering from the light nuclei ^{14}N and ^{16}O enables an average geometry optical model potential to be determined, the strength parameters of which show a smooth behaviour with projectile energy.

1. Introduction

Over the past 15 years, optical model analyses of proton elastic scattering from heavy nuclei (e.g. $A > 40$) have been very successful in fitting the differential cross-section data up to 60 MeV projectile energy. Furthermore, such success has been obtained using potential geometries and parameter values that have systematic trends with target mass and projectile energy variations (Buck 1963; Perey 1963; Bechetti and Greenlees 1969). In contrast, optical model analyses of proton elastic scattering from light nuclei, and particularly from the very light nuclei such as ^{12}C, ^{14}N and ^{16}O, have yielded rather poor quality fits to the data and have often required quite strange and fluctuating (with energy) parameter values. These parameter fluctuations were especially obvious in the early analyses of low energy scattering from ^{12}C (Nodvik *et al.* 1962; Rosen *et al.* 1962). Subsequent analyses of these ^{12}C data (Craig *et al.* 1966; Sprickmann and Geramb 1973) correlated the irregular non-monotonic energy dependences of optical model parameters with resonance effects, as did analyses of elastic scattering data from ^{16}O (Greaves *et al.* 1969; Karban *et al.* 1969). Resonance corrections to the scattering amplitudes also usually yielded markedly improved fits to the data, particularly at large scattering angles where the optical model potential scattering predictions are only a few millibarns per steradian in strength.

In most previous studies of resonance corrections to optical model transitions, the corrections have been sought either after making 'best' optical model fits to all data (Lowe and Watson 1967; Girod *et al.* 1970) or with a fixed energy-independent optical potential (Tamura and Terasawa 1964). In the former method, the optical potential is being forced to reproduce data structures that contain significant resonance effects, while the inverse is true in the latter. In the present analyses, however, we have attempted to be more consistent. We assume that an optical potential of fixed geometry is valid and demand a smooth energy variation in its strength parameters. Such an energy variation is determined by analyses of forward angle data, namely for $\theta < 100°$, and these data usually exceed 8 $\mathrm{mb\,sr^{-1}}$ in magnitude. This scattering region is assumed to be essentially described by the potential scattering aspect of elastic scattering; an assumption based upon the expectation, from parity and angular momentum considerations, that resonance contributions will be symmetric about 90° in the centre of mass system, thereby being most important at large scattering angles where potential scattering is relatively weak. Hence, while resonance contributions should influence predictions at all angles, they will do so with a strength comparable with that observed in large angle data, namely a few millibarns per steradian.

Once the optical potential details have been set we supplement the resultant potential scattering amplitudes with resonance scattering amplitudes of a Breit–Wigner type, as has been formally derived (Feshbach 1962; Feshbach *et al.* 1969), and use a least square search procedure to determine the resonance parameters. Alternative smooth variations of the potential parameters are then used and the above process is repeated to achieve a modicum of self-consistency.

While all available data were analysed by the present optical model analyses, only subsets were chosen to seek resonance corrections. At the higher projectile energies, the optical model analyses by themselves were sufficient to reproduce most of the observed structure and no attempt was made to seek the required small modifications. On the other hand, at the lower projectile energies, the data probably reflect influences of the opening of various reaction channels (Daehnik 1964) and, as such phenomena are not included specifically in our analyses, we did not proceed beyond defining the appropriate optical potential. Hence resonance corrections were applied in analyses of data essentially for projectile energies in the range 20–40 MeV. Such an energy range is particularly interesting since we can expect that the resonance contributions relate dominantly to the virtual excitation of giant resonances in the targets (Sprickmann and Geramb 1973).

In Section 2, the optical model analyses are described, while the effects of resonance corrections are discussed in Section 4.

2. Average Optical Model Potentials

It is now standard practice to take the nuclear optical model potential to be comprised of real and imaginary parts, as

$$V(r) = U(r)+\mathrm{i}W(r), \tag{1}$$

where

$$\begin{aligned} U(r) = {} & V_{\mathrm{C}}(r) - V_0\left\{1+\exp\left(\frac{r-r_0 A^{\frac{1}{3}}}{a_0}\right)\right\}^{-1} \\ & +\boldsymbol{\sigma}.\boldsymbol{l}\, V_{\mathrm{so}}\left(\frac{\hbar}{2m_{\mathrm{p}}c}\right)^2 \frac{1}{r}\frac{\mathrm{d}}{\mathrm{d}r}\left\{1+\exp\left(\frac{r-r_{\mathrm{so}} A^{\frac{1}{3}}}{a_{\mathrm{so}}}\right)\right\}^{-1} \end{aligned} \tag{2}$$

and

$$\begin{aligned} W(r) = {} & -W_{\mathrm{s}}\left\{1+\exp\left(\frac{r-r_{\mathrm{I}} A^{\frac{1}{3}}}{a_{\mathrm{I}}}\right)\right\}^{-1} + 4a_{\mathrm{I}}\, W_{\mathrm{d}}\frac{\mathrm{d}}{\mathrm{d}r}\left\{1+\exp\left(\frac{r-r_{\mathrm{I}} A^{\frac{1}{3}}}{a_{\mathrm{I}}}\right)\right\}^{-1} \\ & +\boldsymbol{\sigma}.\boldsymbol{l}\, W_{\mathrm{so}}\left(\frac{\hbar}{2m_{\mathrm{p}}c}\right)^2 \frac{1}{r}\frac{\mathrm{d}}{\mathrm{d}r}\left\{1+\exp\left(\frac{r-r_{\mathrm{so}} A^{\frac{1}{3}}}{a_{\mathrm{so}}}\right)\right\}^{-1}. \end{aligned} \tag{3}$$

Here $V_{\mathrm{C}}(r)$ is the Coulomb potential of a uniformly charged sphere of total charge

Ze and radius $R_C = r_C A^{\frac{1}{3}}$, that is,

$$V_C(r) = (Zze^2/2R_C)(3 - r^2/R_C^2) \qquad \text{for} \qquad r \leqslant R_C, \tag{4a}$$

$$= Zze^2/r \qquad\qquad r > R_C, \tag{4b}$$

ze being the charge on the incident particle; V_0 is the central strength of the real (or refracting) part of the potential whose range and diffusivity are denoted by r_0 and a_0 respectively, while W_s and W_d are the (imaginary) volume and surface absorptions respectively, each having the same associated radius r_I and diffusivity a_I.

Table 1. Average optical model parameters

The absorption diffusivity a_I was 0·30 fm for ^{14}N, except for the two highest energies, and 0·45 fm for ^{16}O. Apart from these differences the fixed geometry was the same for both cases, namely: r_0 = 1·14 fm, a_0 = 0·68 fm, r_I = 1·40 fm

E (MeV)	V_0 (MeV)	W_s (MeV)	W_d (MeV)	E (MeV)	V_0 (MeV)	W_s (MeV)	W_d (MeV)
			(*a*) ^{14}N				
14·5	61·33	—	8·20	29·8	48·24	2·50	6·30
18·0	57·03	—	8·10	31·0	47·70	5·20	3·90
21·0	53·26	—	8·05	36·6	45·55	6·57[A]	—
23·0	50·93	—	8·00	40·0	44·19	6·71[A]	—
26·0	49·67	—	8·00				
			(*b*) ^{16}O				
14·5	54·5	0·0	5·10	21·4	52·8	8·40	0·45
14·7	54·4	0·0	5·10	22·1	52·7	9·20	0·10
15·2	54·3	0·0	5·10	23·4	52·5	10·05	0·0
15·6	54·2	0·0	5·10	24·3	52·3	10·30	0·0
16·0	54·1	0·0	5·10	24·5	52·2	10·35	0·0
16·4	54·0	0·0	5·10	25·46	52·0	10·35	0·0
17·0	53·8	0·0	5·10	26·2	51·8	10·35	0·0
17·4	53·7	0·0	5·10	27·3	51·6	10·37	0·0
18·0	53·6	0·0	5·10	30·1	51·0	10·40	0·0
18·4	53·5	0·0	5·10	30·5	50·8	10·40	0·0
19·2	53·3	0·0	5·00	34·1	50·0	10·40	0·0
19·8	53·2	2·40	4·60	36·8	49·4	10·40	0·0
20·4	53·1	6·00	2·20	39·7	48·8	10·40	0·0
20·8	53·0	7·10	1·25				

[A] Potential required a_I = 0·68 fm, that is, equal to a_0.

In this work, the Coulomb radius r_C was set to the fixed value of 1·24 fm, not only because the results are not too sensitive to its exact value but also because this value reproduces the experimental Coulomb shift for a $1p_{1/2}$ and $1p_{3/2}$ single-particle bound state. The spin–orbit potential parameters throughout were set to the values 5·4 MeV, 0 MeV, 1·20 fm and 0·6 fm for V_{so}, W_{so}, r_{so} and a_{so} respectively (although V_{so} = 6 MeV is perhaps better for ^{16}O). This standard set was chosen since only differential cross-section data were analysed and the spin–orbit potential has little effect on predictions of data in this form. The spin–orbit potential does strongly influence predictions of polarization but such measurements are scarce for elastic scattering on ^{14}N and of too limited a range for elastic scattering from ^{16}O.

As noted in the Introduction, only the data forward of 100° were used in our searches (chi-square minimization) to determine the optical model potential. Our procedure in achieving this was to first seek the most appropriate geometries, by a literature survey as well as initial optical model search calculations. Once this fixed geometry was established, the various strength parameters as well as the type of absorption (pure volume W_s, pure surface W_d or a combination of both) were sought by further optical model search calculations. The results were then studied as a function of projectile energy and, after repeat runs allowing slight modifications to the geometry, a smooth energy-dependent potential was deduced. The optimum values are shown in Tables 1 for ^{14}N and ^{16}O.

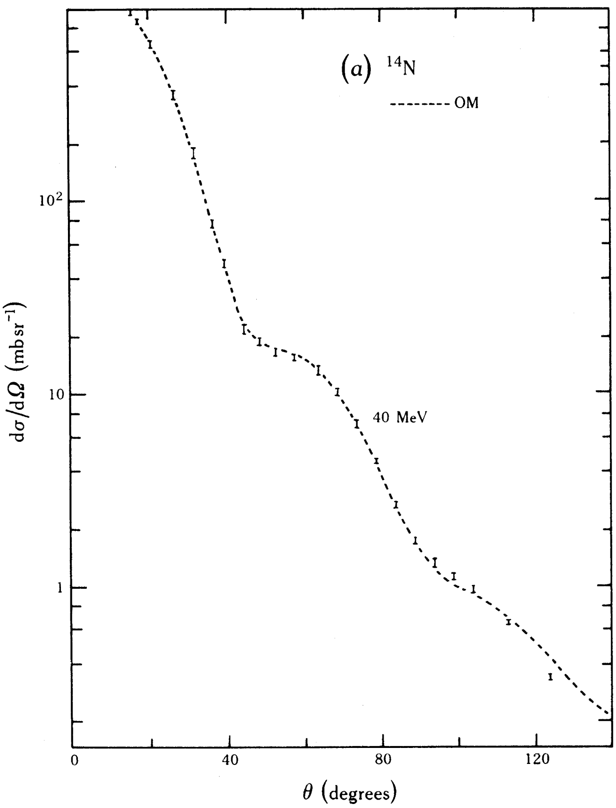

Figs 1*a* and 1*b*. Comparisons of predicted differential cross sections from the optical model (OM) with experimental data for the elastic scattering of (*a*) 40·0 MeV and (*b*) 14·6–36·6 MeV protons from ^{14}N. Resonance-corrected (R) fits are shown by solid curves in (*b*).

It is to be noted that at the higher energies for ^{14}N, where purely volume absorption is optimum, the required associated diffusivity was equal to that of the real part of the optical model potential (our computer code did not allow separate variation of the volume and surface absorption geometries). Such a change was not essential in the ^{16}O analyses. An explanation of this distinction or of the differences in the values of the parameter a_I for ^{14}N and ^{16}O has not been pursued here.

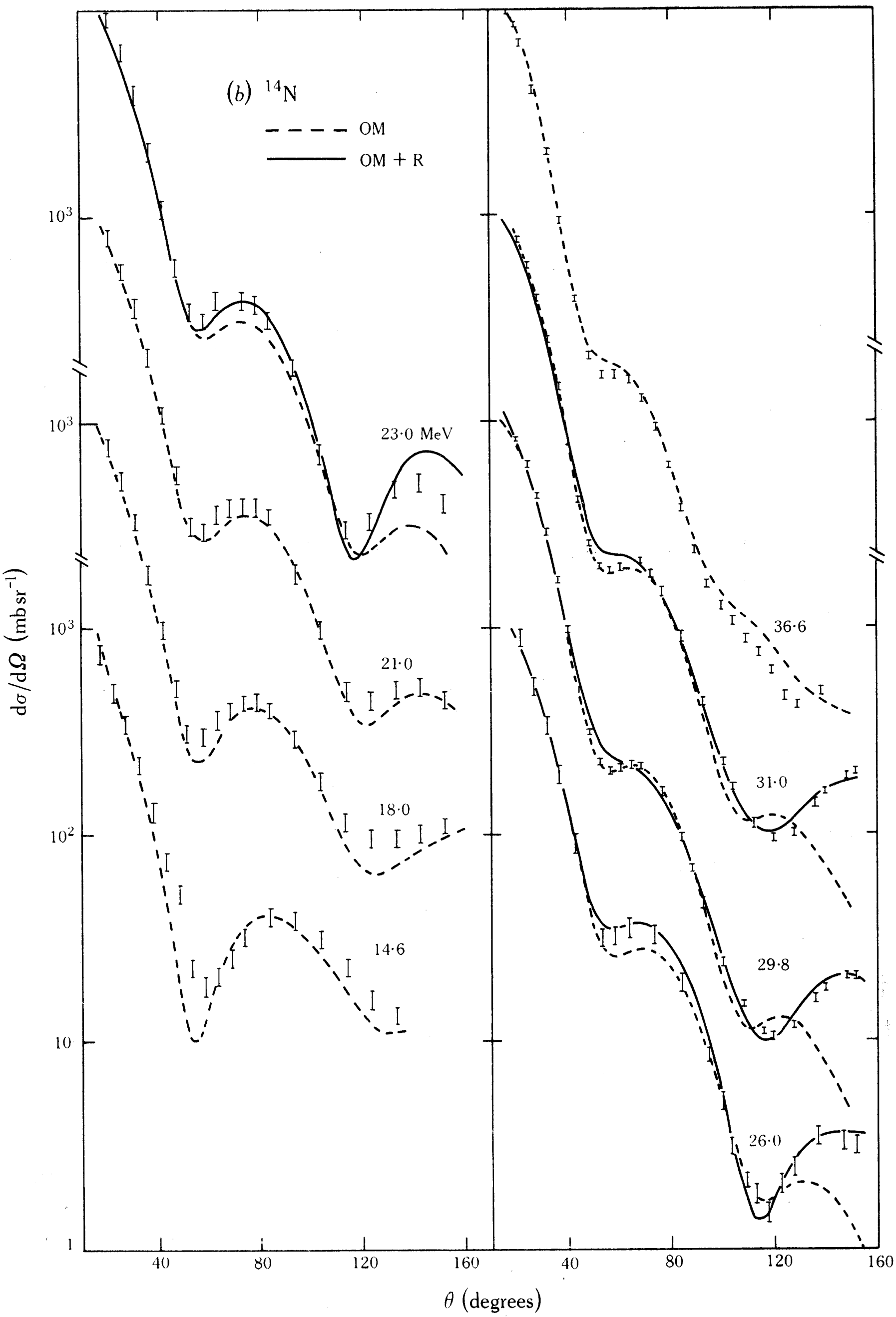

Fig. 1b [*see caption on facing page*]

(*a*) *Optical Model Results for* ^{14}N

Measurements of the differential cross sections for proton elastic scattering from ^{14}N have been made for projectile energies in the range 14–40 MeV at approximately 4 MeV intervals (Kim *et al.* 1964; Curtis *et al.* 1971; Lutz *et al.* 1972; Hansen *et al.* 1973; Fox 1974). This reaction is unusual in that the ground state spin–parity assignment of ^{14}N is 1^+, a fact which could influence potential scattering if a spin–spin term in the optical potential were necessary and significant. The effects of a spin–spin potential have been sought in analyses of the elastic scattering of polarized nucleons from oriented targets by Davies and Satchler (1964) but, as their work deemed such a term to be insignificant, we have not included it in the present studies.

Using the procedure described above, our optical model analyses gave an energy variation in V_0 that was smooth and monotonic but not completely linear. In fact the simplest representation (of the rather sparse data, it must be noted) was a linear decrease of V_0 with E until about 21 MeV whence a change in gradient and a further linear decrease with energy. Smooth variations with energy of the absorptive potential strengths are also apparent from Table 1*a*, albeit that, since the diffusivity of the volume absorption was allowed to increase for the 36·6 and 40 MeV data analyses, it is the volume integral $I(W_{\rm d})$, given by

$$I(W_{\rm d}) = \frac{\partial}{\partial R_{\rm I}}\left\{\frac{4\pi R_{\rm I}^3\, W_{\rm d}}{3}\left(1+\frac{\pi^2 a_{\rm I}^2}{R_{\rm I}^2}\right)\right\}, \qquad \text{with} \qquad R_{\rm I} = r_{\rm I} A^{\frac{1}{3}},$$

that varies smoothly.

The differential cross sections resulting from these optical model calculations are compared with the experimental data in Figs 1*a* and 1*b*. In Fig. 1*a* the 40 MeV results are shown to be in excellent agreement with the data, while in Fig. 1*b* the 14·6–36·6 MeV results shown by the dashed curves reveal a systematic disparity with the data at large scattering angles.

(*b*) *Optical Model Results for* ^{16}O

There are considerably more results for the elastic scattering of protons from ^{16}O in the projectile energy range 14–40 MeV than from ^{14}N. The data exist in about 1 MeV steps (Kobayashi 1960; Daehnik 1964; Cameron *et al.* 1968; Karban *et al.* 1969) thus providing a better test for an average field specification than the ^{14}N data. Nevertheless, the geometry of the ^{14}N potential was used as the first guess for the ^{16}O analyses and, except that the absorption diffusivity had to be altered to a value of 0·45 fm, it was found to be completely adequate.

Again by limiting the data to which fits were sought to those forward of 100°, smooth variations in the potential strengths were found in general. The real potential strength varied smoothly and linearly with energy over the entire range (Table 1*b*). The absorptive potential strengths also show a smooth variation with energy and, as in the ^{14}N case, a transition from pure surface to pure volume type occurs but now in the region of 19–22 MeV projectile energy. However, in the energy range 14–18 MeV, strong fluctuations in $W_{\rm d}$ are required to fit the data; this requirement was also noted in the analyses of Daehnik (1964) as well as that of Duke (1963) and was attributed to the several reaction thresholds existing in this energy region. In fact, Daehnik observed strong fluctuations in data at 13·35, 14·85 and 16·9 MeV and 12 other lesser fluctuations in the 13–19 MeV range.

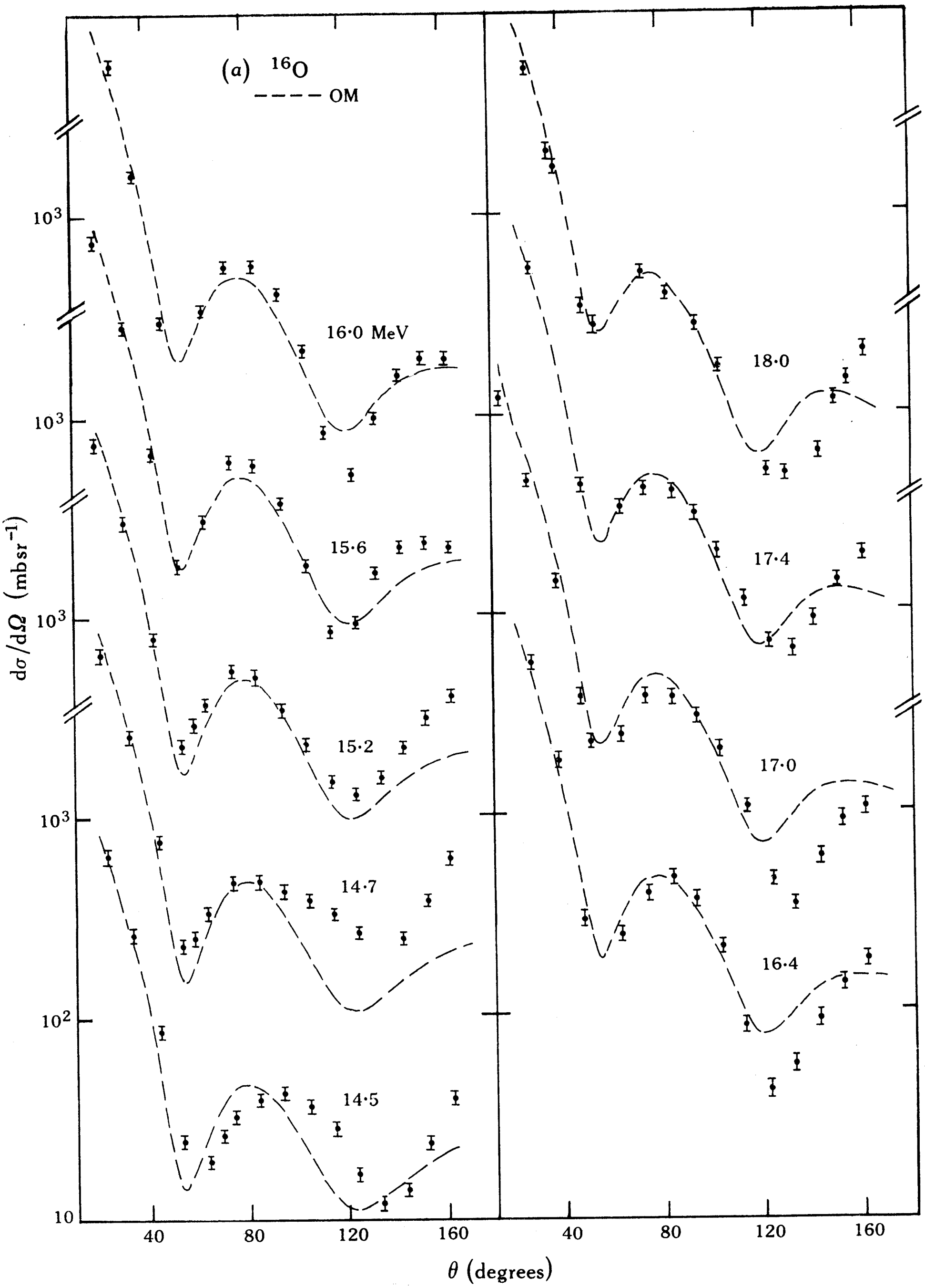

Figs 2a–2d (pp. 293–6). Comparisons of predicted differential cross sections from the optical model (OM) with experimental data for the elastic scattering of 14·5–39·7 MeV protons from ^{16}O. Resonance-corrected (R) fits are shown by solid curves in (b) and (c).

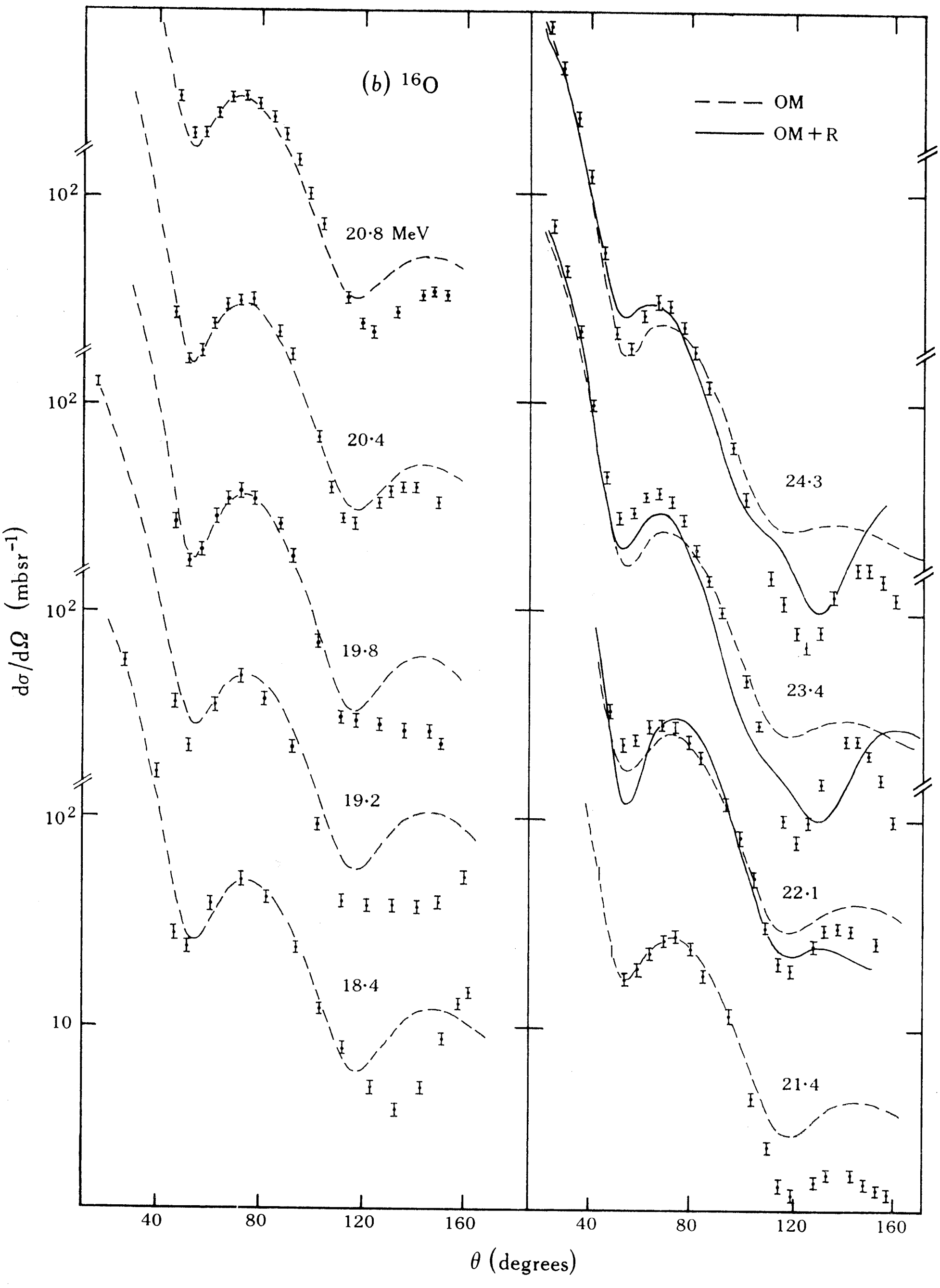

Fig. 2*b*. $E_p = 18{\cdot}4$–$24{\cdot}3$ MeV

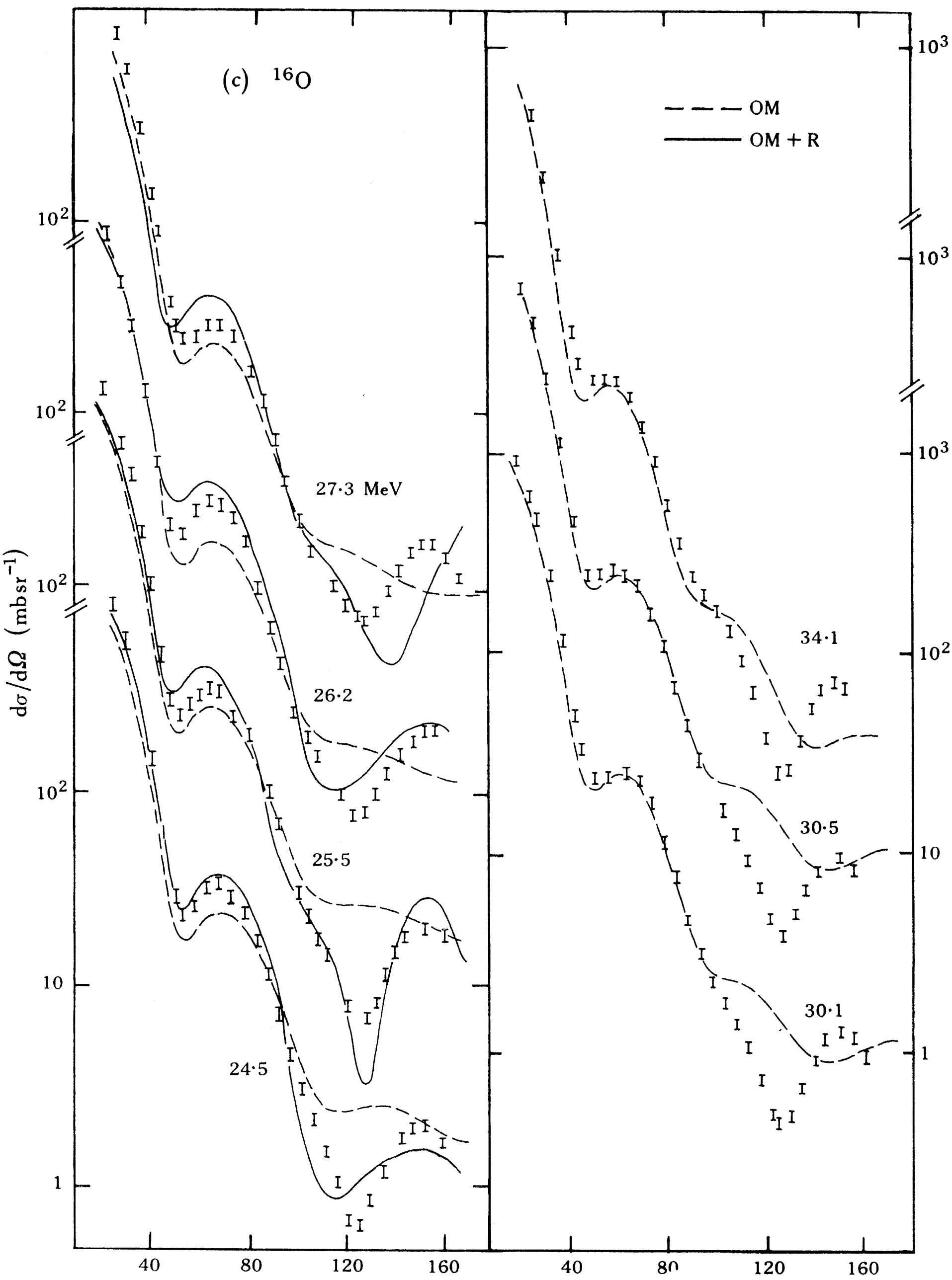

Fig. 2c. $E_p = 24 \cdot 5$–$34 \cdot 1$ MeV

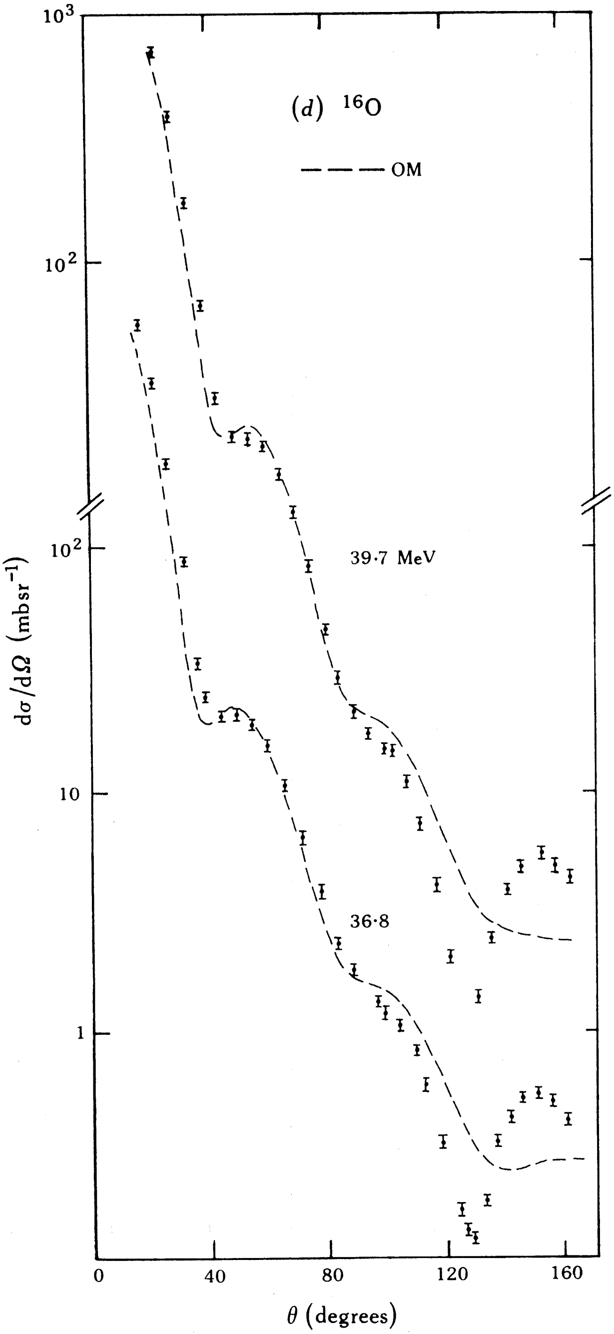

Fig. 2*d*. E_p = 36·8 and 39·7 MeV

The optical model predictions obtained here are compared with the experimental data in Figs 2*a*–2*d* (dashed curves). In the 14·5–18·0 MeV results (Fig. 2*a*) there is a rapid fluctuation of data about the average potential results at large scattering angles, which is characteristic of the opening of reaction channels. The disparities between the data and the optical potential results for 18·4–34·1 MeV (Figs 2*b* and 2*d*) are again most evident at the large scattering angles, but they now show a regular trend with projectile energy. Finally, the predictions agree well with the 36·8 and 39·7 MeV data (Fig. 2*d*), save for the large-angle region, but the data (and predictions) here have very small magnitude.

(*c*) *Optical Parameter Comparisons*

Because of the small range of energies studied in the past by any one author, it is not possible to satisfactorily compare previous energy dependences of the ^{14}N absorptive potentials W_s and W_d with those obtained in the present work. However, one may compare the geometry deduced herein with those used in the past. The previous values of a_I seem to be slightly higher than ours, particularly at low energies. Apart from this difference our values lie well within the limits of those obtained by others. Likewise the optical parameters obtained in the recent past for ^{16}O agree well with the present geometry.

There have been a number of quite extensive studies made of the energy dependence of the real part of the central potential. Buck (1963) analysed proton elastic and inelastic scattering in the energy range 10–20 MeV for medium mass targets and obtained the energy dependence

$$V_0 = 52\cdot6 - 0\cdot28\,E \pm 1\cdot0 \qquad \text{MeV}. \tag{5}$$

Perey (1963) added an extra term to account for the decrease in the kinetic energy of the proton inside the nucleus caused by the Coulomb potential, and obtained

$$V_0 = 53\cdot3 - 0\cdot55\,E + \{0\cdot4(Z/A^{\frac{1}{3}}) + 27(N-Z)/A\} \qquad \text{MeV}. \tag{6}$$

Later surveys determined other variations: notably an analysis of 30–40 MeV data by Fricke *et al.* (1967) resulted in the variation

$$V_0 = 49\cdot9 - 0\cdot22\,E + 0\cdot4\,Z/A^{\frac{1}{3}} + 26\cdot4(N-Z)/A\,, \tag{7}$$

while that for $A > 40$ by Bechetti and Greenlees (1969) yielded

$$V_0 = 55\cdot2 - 0\cdot32\,E + 0\cdot27\,Z/A^{\frac{1}{3}} + 24(N-Z)/A\,. \tag{8}$$

If each of the above variations (6), (7) and (8) are extrapolated to the ^{16}O case then the expected variations of V_0 with energy are

$$V_0 = 54\cdot6 - 0\cdot55\,E, \quad V_0 = 51\cdot2 - 0\cdot22\,E \quad \text{or} \quad V_0 = 56\cdot0 - 0\cdot32\,E. \tag{9}$$

The results of our analyses yield

$$V_0 = 78\cdot8 - 0\cdot22\,E \qquad \text{for} \qquad E < 21\ \text{MeV}, \tag{10a}$$

$$= 60\cdot0 - 0\cdot4\,E \qquad\qquad E > 21\ \text{MeV} \tag{10b}$$

and

$$V_0 = 57\cdot8 - 0\cdot23\,E \tag{11}$$

for the ^{14}N and ^{16}O cases respectively.

3. Addition of Resonance Corrections

While the optical model calculations of elastic scattering from ^{14}N agree well with the data at forward angles ($\theta < 100°$) for all the energies analysed, there are discrepancies at backward angles, notably for 23·0, 26·0, 29·8 and 31·0 MeV incident proton energies, and these discrepancies are characteristic of a resonance amplitude interfering with that of potential scattering. Since the magnitude of the differences between the experimental data and the potential scattering predictions is approximately 3 mb sr^{-1} at back angles, where the cross section is about 10 mb sr^{-1}, it should be possible theoretically to correct this discrepancy without having a large effect on the forward angle fit, where the cross section is typically of the order of hundreds of millibarns per steradian. The fits for the ^{16}O data showed similar trends, with back-angle differences between the data and the predictions at most energies from 22·1 to 39·7 MeV, the magnitude of the differences in this case being around 6 mb sr^{-1}. Although the average optical model potential did not produce an exceptionally good fit in the 14·5–18·4 MeV energy range for ^{16}O, it was decided not to attempt a resonance correction at these energies because of the multiplicity of reactions that have their onset in this region.

The energies of the compound systems ^{15}O and ^{17}F were obtained by adding the separation energy gained (when the proton and target nucleus temporarily amalgamate) to the incident proton energy in the centre of mass system. The separation energy gain was of a significant magnitude only for ^{14}N, for which the value was 7·293 MeV (Ajzenberg-Selove 1970); for ^{16}O the energy gain of 0·601 MeV (Ajzenberg-Selove 1971) barely offsets the centre of mass correction to the laboratory energy. Thus, for scattering from ^{14}N, the obvious disparities in the data taken with projectile energies of 23·0, 26·0, 29·8 and 31·0 MeV are associated with excitation energies in ^{15}O of 28·8, 31·5, 35·1 and 36·2 MeV respectively whereas, for scattering from ^{16}O, the observed large-angle disparities between the data and the optical model predictions for proton energies from 23·4 to 27·3 MeV coincide with excitation energies in ^{17}F between 22·6 and 26·3 MeV.

(a) *Form of Resonance Corrections*

The general scattering amplitudes for spin $\frac{1}{2}$ particles scattering from a zero spin target have the form

$$S(\theta) = A(\theta) + B(\theta)\,\boldsymbol{\sigma}.\hat{\boldsymbol{n}}\,, \tag{12}$$

where $\hat{\boldsymbol{n}}$ is the unit normal to the scattering plane. From this, the differential cross section can be expressed as

$$\mathrm{d}\sigma/\mathrm{d}\Omega = |A(\theta)|^2 + |B(\theta)|^2 = \sigma(\theta)\,. \tag{13}$$

Optical model results are then energy-averaged predictions of the scattering amplitudes A and B with an energy-averaging interval of the order of mega-electronvolts (Feshbach *et al.* 1969), whence

$$A(\theta) \to \langle A(\theta)\rangle_{\mathrm{MeV}} = f_{\mathrm{C}}(\theta) + k^{-1}\sum_l \exp(2\mathrm{i}\sigma_l)\,\mathrm{P}_l(\theta) \times [(l+1)\exp(\mathrm{i}\delta_{l+})\sin\delta_{l+} + l\exp(\mathrm{i}\delta_{l-})\sin\delta_{l-}] \tag{14}$$

and

$$B(\theta) \rightarrow \langle B(\theta)\rangle_{\mathrm{MeV}} = -\mathrm{i}k^{-1}\sum_{l}\exp(2\mathrm{i}\sigma_l)\,\mathrm{P}_l(\theta)$$
$$\times[\exp(\mathrm{i}\delta_{l+})\sin\delta_{l+} - \exp(\mathrm{i}\delta_{l-})\sin\delta_{l-}]\,, \qquad (15)$$

where $f_{\mathrm{C}}(\theta)$ denotes the Coulomb scattering amplitude and the $l\pm$ subscripts indicate $\mathscr{J}$ values of $l\pm\frac{1}{2}$. All other quantities are in standard notation.

Inherent in the above prescription is an inability to explain data variation over energy intervals less than the average. However, by using the Feshbach prescription and smaller energy-averaging intervals, it is possible to deduce that the average scattering amplitudes $\langle A\rangle$ and $\langle B\rangle$ of equations (14) and (15) should remain and be supplemented by energy-varying contributions that coincide with doorway-state participation in the transitions but yet average out rapid fluctuations of compound nuclear nature. Thus data variation with energy in intervals of the order of kilo-electronvolts can be interpreted by this doorway-state hypothesis, the required 'resonance' amplitudes then being

$$A_{\mathrm{R}}(\theta) = (2\mathrm{i}k)^{-1}\sum_{l}\exp(2\mathrm{i}\sigma_l)\,\mathrm{P}_l(\theta)\,[(l+1)T_{\mathrm{R}}^{(+)}(\alpha\, l\tfrac{1}{2}) + l\,T_{\mathrm{R}}^{(-)}(\alpha\, l\tfrac{1}{2})]\,, \qquad (16)$$

$$B_{\mathrm{R}}(\theta) = -(2k)^{-1}\sum_{l}\exp(2\mathrm{i}\sigma_l)\,\mathrm{P}_l(\theta)\,[T_{\mathrm{R}}^{(+)}(\alpha\, l\tfrac{1}{2}) - T_{\mathrm{R}}^{(-)}(\alpha\, l\tfrac{1}{2})]\,, \qquad (17)$$

where, following the Feshbach formalism, the amplitudes

$$T_{\mathrm{R}}^{(\pm)}(\alpha\, l\tfrac{1}{2}) = -\exp(2\mathrm{i}\delta_{l\pm})\,(g_{d\alpha})^2/\{E-\varepsilon_d(J_d)+\tfrac{1}{2}\mathrm{i}\Gamma_{\mathrm{d}}(J_d)\} \qquad (18)$$

carry the coupling between the elastic channel α and any doorway state d of total angular momentum J_d and energy ε. In order to use the detailed expansion of these resonance scattering amplitudes, it is necessary to have a precise spectroscopy of the doorway states, and since this is lacking we simply treat the amplitudes $T_{\mathrm{R}}^{(\pm)}$ as adjustable complex quantities.

To simplify interpretation of the results we further assume that the doorway states are formed by capture of the projectile into an unoccupied 2s–1d shell orbit l_j, the target response being an excitation to a state (at high energy) of spin and parity J^π; the most obvious of these target response states will be the giant resonances. Hence with targets of spin and parity assignments I^π, we have the constraint

$$\boldsymbol{I}+\boldsymbol{\mathscr{J}} = \boldsymbol{j}+\boldsymbol{J}\,,$$

as well as that of parity conservation. Given a specific giant resonance then we can specify which partial-wave scattering amplitudes could be affected by resonance corrections.

(*b*) *Results and Discussion*

Inclusion of resonance effects enables the optical model predictions to be modified to the forms shown in Figs 1*b*, 2*b* and 2*c* (solid curves). There is a marked improvement in the fits to the data particularly at large angles.

The ^{14}N results required $(l, \mathscr{J})$ resonance corrections to the $(1,3/2)$ and $(2,3/2)$ channels only. The magnitudes of the T_{R} amplitudes are specified in Table 2*a*. Regrettably the data are far too scarce to draw any conclusions. However, the results are consistent with a general background contribution from E1 (isovector dipole) giant resonances and, from the $T_R^{(+)}(\alpha\, 2\tfrac{1}{2})$ values, also strong isoscalar E2 resonance effects.

The resonance-corrected fits to the elastic scattering data from ^{16}O required the T_R amplitudes listed in Table 2*b*. The odd $(l, \mathscr{J})$ corrections (in this case $(1, 1/2)$, $(1, 3/2)$ and $(3, 7/2)$) within our model interpretations reflect the influence of virtual excitation of isovector E1 and isoscalar E3 giant resonances, while the even corrections ($(2, 3/2)$ and $(2, 5/2)$) indicate isoscalar E2 giant resonance properties. In the associated excitation energy (ε_d) range, other studies (Geramb *et al.* 1973; Hanna *et al.* 1974; Breuer *et al.* 1975) have observed fractionated E1 and E2 strengths as we conjecture from our analyses. More finely spaced (in energy) data and complementary measurements of polarizations would be most useful in furthering these analyses.

Table 2. Magnitudes of resonance amplitudes

E_{lab} (MeV)	$T_R^{(-)}(\alpha\, 1\tfrac{1}{2})$	$T_R^{(-)}(\alpha\, 2\tfrac{1}{2})$	$T_R^{(+)}(\alpha\, 1\tfrac{1}{2})$	$T_R^{(+)}(\alpha\, 2\tfrac{1}{2})$	$T_R^{(+)}(\alpha\, 3\tfrac{1}{2})$
			(*a*) ^{14}N		
23·0	—	—	0·314	0·295	—
26·0	—	—	0·392	0·175	—
29·8	—	—	0·395	0·415	—
31·0	—	—	0·390	0·273	—
			(*b*) ^{16}O		
23·4	0·694	0·419	0·308	0·706	0·686
24·3	0·658	0·339	0·802	0·854	0·655
24·5	0·976	0·508	0·205	0·522	0·737
25·46	0·948	0·863	0·557	0·717	0·821
26·2	1·240	0·419	0·170	0·693	0·632
27·3	0·639	0·372	0·660	0·624	0·581

Finally, the disparities at large angles between the optical model predictions and the data for projectile energies of 36·8 and 39·7 MeV are worth further consideration in view of the quite recent analyses of Mackintosh and Kobos (1976), who made a coupled reaction channel analysis of 30 MeV proton scattering from ^{40}Ca. By including deuteron pickup channels specifically, they noted an influence on elastic scattering predictions quite similar to the large-angle data for ^{16}O and in particular to the minima near 135°. Such corrections are small in comparison to the large variations we have sought to analyse but nevertheless should be included in future more sophisticated treatments of data.

4. Conclusions

The results presented here justify the use of an average optical potential model in analyses of scattering from light nuclei and reveal how strong resonance effects influence experimental data. In particular, the role of giant resonances as doorway states in non-potential scattering contributions has been demonstrated and a measure of the importance of their amplitudes in analyses has been obtained.

References

Ajzenberg-Selove, F. (1970). *Nucl. Phys.* A **152**, 1.

Ajzenberg-Selove, F. (1971). *Nucl. Phys.* A **166**, 1.

Bechetti, F. D., and Greenlees, G. W. (1969). *Phys. Rev.* **182**, 1190.

Breuer, H., Knöpfle, K. T., Mayer-Böricke, C., Rugge, M., and Wagner, G. J. (1975). Proc. Int. Symp. on Highly Excited States in Nuclei, Jülich, West Germany (Eds A. Faessler, C. Mayer-Böricke and P. Turek), p. 4.

Buck, B. (1963). *Phys. Rev.* **130**, 712.

Cameron, J. M., Richardson, J. R., van Oers, W. T. H., and Verba, J. W. (1968). *Phys. Rev.* **167**, 908.

Craig, R. M., Dore, J. C., Greenlees, G. W., Lowe, J., and Watson, D. L. (1966). *Nucl. Phys.* **79**, 177.

Curtis, T. H., Lutz, H. F., Heikkinen, D. W., and Bartolini, W. (1971). *Nucl. Phys.* A **165**, 19.

Daehnik, W. W. (1964). *Phys. Rev.* **135**, 1168.

Davies, K. T. R., and Satchler, G. R. (1964). *Nucl. Phys.* **53**, 1.

Duke, C. B. (1963). *Phys. Rev.* **129**, 681.

Feshbach, H. (1962). *Ann. Phys.* (*New York*) **19**, 287.

Feshbach, H., Kerman, A. K., and Lemmer, R. H. (1969). *Ann. Phys.* (*New York*) **41**, 230.

Fox, S. H. (1974). Ph.D. Thesis, Michigan State University.

Fricke, M. P., Gross, E. E., Morton, B. J., and Zucker, A. (1967). *Phys. Rev.* **156**, 1207.

Geramb, H. V., Sprickmann, R., and Strobel, G. L. (1973). *Nucl. Phys.* A **199**, 545.

Girod, M., von Sen, N., Longequeue, J. P., and Chang, T. U. (1970). *J. Phys.* (*Paris*) **31**, 125.

Greaves, P. D., Hnidzo, V., Karban, O., and Lowe, J. (1969). Rutherford Lab. Rep. No. R187, p. 41.

Hanna, S. S., Glavish, H. F., Avida, R., Calarco, J. R., Kuhlmann, E., and La Canna, R. (1974). *Phys. Rev. Lett.* **32**, 114.

Hansen, L. F., Grimes, S. M., Kammerdiener, L. J., and Madsen, V. A. (1973). *Phys. Rev.* C **8**, 2072.

Karban, O., Greaves, P. D., Hnidzo, V., Lowe, J., Berovic, N., and Wojciechowski, H. (1969). *Nucl. Phys.* A **132**, 548.

Kim, C. C., Bunch, S. M., Devins, D. W., and Forster, H. H. (1964). *Nucl. Phys.* **58**, 32.

Kobayashi, S. (1960). *J. Phys. Soc.* (*Jpn*) **15**, 1164.

Lowe, J., and Watson, D. L. (1967). *Phys. Lett.* **24**, 174.

Lutz, H. F., Heikkinen, D. W., and Bartolini, W. (1972). *Nucl. Phys.* A **198**, 257.

Mackintosh, R. S., and Kobos, A. M. (1976). *Phys. Lett.* B **62**, 127.

Nodvik, J. S., Duke, C. B., and Melkanoff, M. A. (1962). *Phys. Rev.* **125**, 975.

Perey, F. G. (1963). *Phys. Rev.* **131**, 745.

Rosen, L., Darriulat, P., Farragi, H., and Garin, A. (1962). *Nucl. Phys.* **33**, 458.

Sprickmann, R., and Geramb, H. V. (1973). Ann. Rep. Inst. Kernphysik, Kernforschungsanlage, Jülich, West Germany, No. P215.

Tamura, T., and Terasawa, T. (1964). *Phys. Lett.* **8**, 41.

Manuscript received 1 December 1976